Reactions of ruthenium and rhodium atoms with carbon monoxide and dinitrogen mixtures: A combined experimental and theoretical study

Ling Jiang, Zhang-Hui Lu, and Qiang Xu

Citation: The Journal of Chemical Physics **132**, 054504 (2010); doi: 10.1063/1.3299715
View online: https://doi.org/10.1063/1.3299715
View Table of Contents: http://aip.scitation.org/toc/jcp/132/5
Published by the American Institute of Physics

Articles you may be interested in

Reactions of molybdenum and tungsten atoms with nitrous oxide in excess argon: A combined matrix infrared spectroscopic and theoretical study
The Journal of Chemical Physics **132**, 164305 (2010); 10.1063/1.3395338

Intermediates of CO oxidation on iron oxides: An experimental and theoretical study
The Journal of Chemical Physics **134**, 034305 (2011); 10.1063/1.3523648

Infrared spectra and density functional theory calculations of the tantalum and niobium carbonyl dinitrogen complexes
The Journal of Chemical Physics **131**, 034512 (2009); 10.1063/1.3186759

Infrared spectroscopic and theoretical studies on the formation of Au_2NO^- and Au_nNO $(n=2-5)$ in solid argon
The Journal of Chemical Physics **130**, 134511 (2009); 10.1063/1.3109689

Theoretical study of the interaction of carbon monoxide with $3d$ metal dimers
The Journal of Chemical Physics **128**, 124317 (2008); 10.1063/1.2842066

Reactions of silicon atoms and small clusters with CO: Experimental and theoretical characterization of $Si_nCO(n=1-5)$, $Si_2(CO)_2$, $c-Si_2(\mu-O)(\mu-CSi)$, and $c-Si_2(\mu-O)(\mu-CCO)$ in solid argon
The Journal of Chemical Physics **121**, 10474 (2004); 10.1063/1.1811078

PHYSICS TODAY
WHITEPAPERS

ADVANCED LIGHT CURE ADHESIVES

Take a closer look at what these environmentally friendly adhesive systems can do

READ NOW

PRESENTED BY
MASTERBOND
ADHESIVES | SEALANTS | COATINGS

THE JOURNAL OF CHEMICAL PHYSICS **132**, 054504 (2010)

Reactions of ruthenium and rhodium atoms with carbon monoxide and dinitrogen mixtures: A combined experimental and theoretical study

Ling Jiang,[1] Zhang-Hui Lu,[1,2] and Qiang Xu[1,2,a)]
[1]*National Institute of Advanced Industrial Science and Technology (AIST), Ikeda, Osaka 563-8577, Japan*
[2]*Graduate School of Engineering, Kobe University, Nada Ku, Kobe, Hyogo 657-8501, Japan*

(Received 13 July 2009; accepted 7 January 2010; published online 3 February 2010)

Laser-ablated Ru and Rh atoms react with CO and N_2 mixture in excess neon to produce the carbonylmetal dinitrogen complexes, $(NN)_nMCO$ (M=Ru,Rh; n=1,2) and $NNRu(CO)_2$, as well as metal carbonyls and dinitrogen complexes. These carbonylmetal dinitrogen complexes are characterized using infrared spectroscopy on the basis of the results of the isotopic substitution and mixed isotopic splitting patterns. Density functional theory calculations have been performed on these complexes. Overall agreement between the experimental and calculated vibrational frequencies, relative absorption intensities, and isotopic shifts supports the identification of these species from the matrix infrared spectra. Furthermore, a plausible reaction pathway for the formation of the products has been proposed. This work reveals that the reactivity of Ru and Rh atoms toward CO is prior to N_2. © *2010 American Institute of Physics*. [doi:10.1063/1.3299715]

I. INTRODUCTION

Reactions under nontraditional experimental conditions can often yield new and exciting species not accessible from normal chemical reaction conditions.[1] Recent studies have shown that, with the aid of isotopic substitution, matrix isolation infrared spectroscopy, combined with quantum chemical calculation, is very powerful in investigating the spectrum, structure, and bonding of novel species and the related reaction mechanisms.[2,3] The interaction of ruthenium and rhodium atoms with small molecules (i.e., CO, O_2, CO_2, H_2, N_2, CH_4, etc.) is of considerable interest due to its importance in many catalytic processes.[4] Among these small molecules, carbon monoxide and dinitrogen are two of the most important in transition-metal chemistry from an academic or an industrial viewpoint.[4,5] For instance, the rhodium dicarbonyl on alumina, silica, and zeolites is widely used as a catalyst system for activation of many molecules including N_2, H_2, CO_2, and alkanes[6–11] through a coordinatively unsaturated $Rh^I(CO)$ center. Previous investigations exhibit that the adsorption of dinitrogen molecules on supported rhodium carbonyls produces the $Rh(CO)(N_2)$ species.[7,12] Theoretically, $Rh(CO)(N_2)$ is predicted to have a bent structure with a $^2A'$ ground state.[13] Similarly, the $Ru(CO)_x$ (x=1,2) complexes react with dihydrogen molecules to generate the ruthenium carbonyl dihydride $H_2Ru(CO)_2$ and the hydrogen complexes $(H_2)_xRuCO$ (x=1,2).[14]

In contrast with extensive experimental and theoretical investigations of the interaction of Rh and Ru atoms with separate CO or N_2 molecules,[15–22] however, much less work has been done on the simultaneous interaction of these metal atoms with CO and one countermolecule N_2. In this paper, we report a combined matrix isolation infrared spectroscopic and theoretical study of the reactions of laser-ablated Ru and Rh atoms with CO/N_2 mixtures in excess neon. IR spectroscopy coupled with theoretical calculation provides evidence for the formation of the carbonylmetal dinitrogen complexes, $(NN)_nMCO$ (M=Ru,Rh; n=1,2) and $NNRu(CO)_2$, and the reactivity of Ru and Rh atoms toward CO is prior to N_2.

II. EXPERIMENTAL AND THEORETICAL METHODS

The experiments for laser ablation and matrix isolation infrared spectroscopy are similar to those previously reported.[23] In short, the neodymium-doped yttrium aluminum garnet laser fundamental (1064 nm, 10 Hz repetition rate with 10 ns pulse width) was focused on the rotating Ru and Rh targets. The laser-ablated metal atoms were codeposited with CO/N_2 mixtures in excess neon onto a CsI window cooled normally to 4 K by means of a closed-cycle helium refrigerator. Typically, 1–30 mJ/pulse laser power was used. CO (99.95%, Japan Fine Products), $^{13}C^{16}O$ (99%, ^{18}O <1%, ICON), $^{12}C^{18}O$ (99%, ICON), N_2 (99.95%, SUZUKI SHOKAN Co., Ltd.), $^{15}N_2$ (99.8%, SHOKO Co., Ltd.), and mixed isotopic samples were used to prepare the $CO/N_2/Ne$ mixtures. In general, matrix samples were deposited for 30–60 min with a typical rate of 2–4 mmol/h. After sample deposition, IR spectra were recorded on a BIO-RAD FTS-6000e spectrometer at 0.5 cm^{-1} resolution using a liquid nitrogen cooled HgCdTe (MCT) detector for the spectral range of 5000–400 cm^{-1}. Samples were annealed at different temperatures and subjected to broadband irradiation (λ >250 nm) using a high-pressure mercury arc lamp (Ushio, 100 W).

Quantum chemical calculations were performed to predict the structures and vibrational frequencies of the observed reaction products using the GAUSSIAN 03 program.[24] The B3-LYP exchange correlation functional was used.[25] The 6–311+G(d) basis set was used for the C, O, and N atoms,[26] and the scalar-relativistic Stuttgart-Dresden (SDD) pseudo-

---

[a)] Author to whom correspondence should be addressed. Electronic mail: q.xu@aist.go.jp.

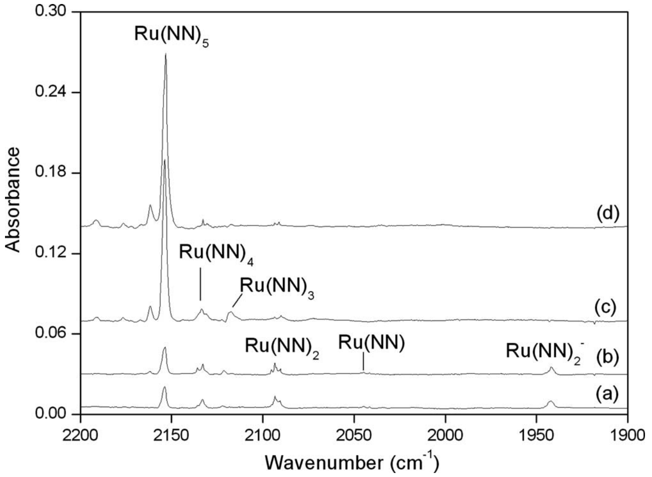

FIG. 1. Infrared spectra in the 2200–1900 cm^{-1} region from codeposition of laser-ablated Ru atoms with 0.4% N_2 in Ne. (a) 40 min of sample deposition at 4 K, (b) after annealing to 6 K, (c) after 10 min of broadband irradiation, and (d) after annealing to 10 K.

potential and basis set were used for the Ru and Rh atoms.[27] Geometries were fully optimized and vibrational frequencies were calculated with analytical second derivatives. Recent investigations have shown that such computational methods can provide reliable information for metal complexes, such as infrared frequencies, relative absorption intensities, and isotopic shifts.[15–23]

III. RESULTS AND DISCUSSION

Experiments have been done with CO and N_2 concentrations ranging from 0.05% to 5.0% in excess neon. Typical infrared spectra for the reactions of laser-ablated Ru and Rh atoms with CO and N_2 molecules in excess neon in the selected regions are illustrated in Figs. 1–6, and the absorption bands in different isotopic experiments are listed in Tables I and II. The stepwise annealing and photolysis behavior of the product absorptions is also shown in the figures and will be discussed below. Meanwhile, experiments have also been done for the codeposition of laser-ablated Ru and Rh atoms with separated CO and N_2 samples to confirm the new absorptions. While the $Ru(CO)_x$ ($x=1-5$), $Rh(CO)_y$, and $Rh(NN)_y$ ($y=1-4$) complexes have been characterized in solid neon,[17–19,21,22] the $Ru(NN)_x$ ($x=1-5$) complexes have only been reported in argon and pure nitrogen matrices.[20] Prior to the discussion of the carbonylmetal dinitrogen complexes, brief assignments for $Ru(NN)_x$ in neon matrix will be given in Sec. III A. Only infrared spectra from the reactions of Ru atoms with pure N_2 in neon matrix are shown here (Figs. 1 and 2).

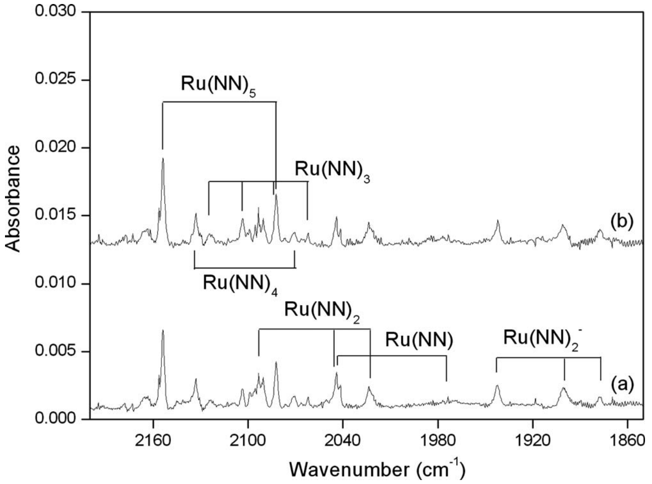

FIG. 2. Infrared spectra in the 2160–1860 cm^{-1} region for laser-ablated Ru atoms codeposited with 0.2% $^{14}N_2$+0.2% $^{15}N_2$ mixtures in Ne. (a) 40 min of sample deposition at 4 K and (b) after annealing to 6 K.

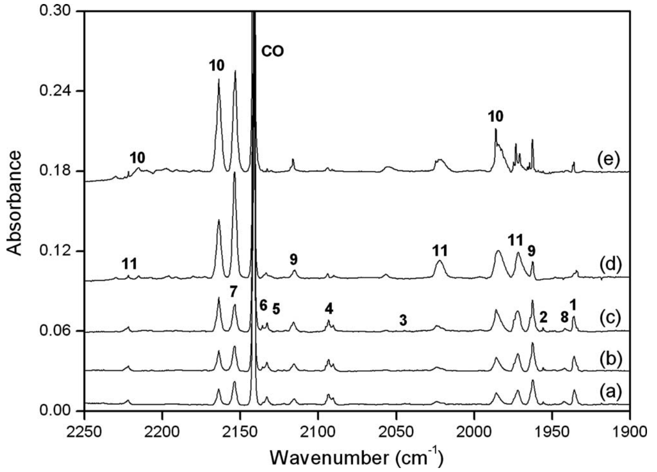

FIG. 3. Infrared spectra in the 2250–1900 cm^{-1} region from codeposition of laser-ablated Ru atoms with 0.1%CO+0.5%N_2 in Ne. (a) 40 min of sample deposition at 4 K, (b) after annealing to 6 K, (c) after annealing to 8 K, (d) after 10 min of broadband irradiation, and (e) after annealing to 10 K.

Density functional theory (DFT) calculations have been carried out for the possible isomers and electronic states of the potential product molecules. Figure 7 shows the most stable structures of the new products. The ground electronic states, point groups, vibrational frequencies, and intensities are listed in Table III. Table IV reports a comparison of the

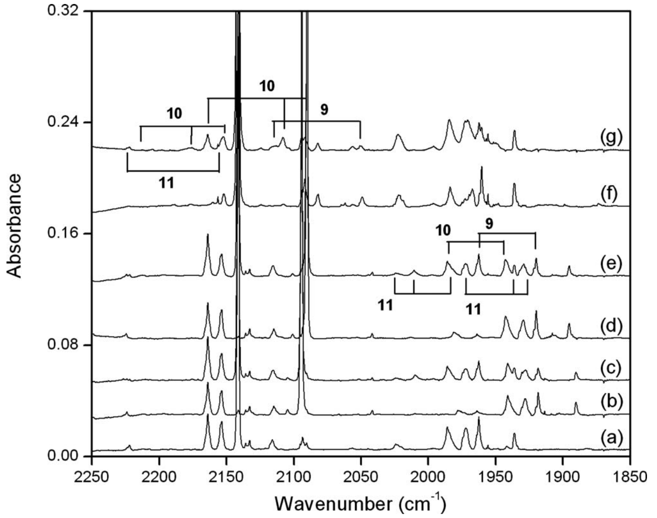

FIG. 4. Infrared spectra in the 2250–1850 cm^{-1} region for laser-ablated Ru atoms codeposited with isotopic CO/N_2 mixtures in Ne after annealing to 8 K. (a) 0.1%CO+0.5%N_2, (b) 0.1%^{13}CO+0.5%N_2, (c) 0.08%^{12}CO+0.08%^{13}CO+0.5%N_2, (d) 0.1%$C^{18}O$+0.5%N_2, (e) 0.08%$C^{16}O$+0.08%$C^{18}O$+0.5%N_2, (f) 0.1%CO+0.5% $^{15}N_2$, and (g) 0.1%CO+0.4% $^{14}N_2$+0.4% $^{15}N_2$.

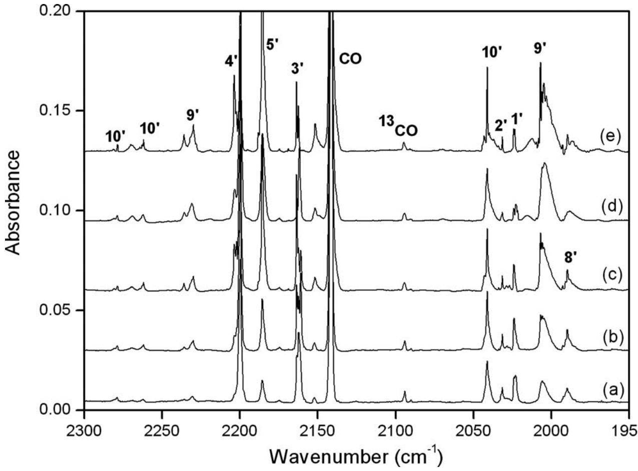

FIG. 5. Infrared spectra in the 2300–1950 cm^{-1} region from codeposition of laser-ablated Rh atoms with 0.1%CO+0.4%N$_2$ in Ne. (a) 1 h of sample deposition at 4 K, (b) after annealing to 8 K, (c) after annealing to 10 K, (d) after 10 min of broadband irradiation, and (e) after annealing to 12 K.

experimental and calculated isotopic frequency ratios for the N–N and C–O stretching modes of the new products. Molecular orbital analysis has been performed to address the bonding mechanism in these new products. It has been found that the bonding mechanisms of Rh system are similar to those of Ru system. Then, only the representative molecular orbitals of Ru system are presented in Fig. 8.

A. Ru(NN)$_x$(x=1–5) and Ru(NN)$_2^-$

In the reactions of Ru atoms with pure N$_2$ in neon matrix (Figs. 1 and 2), absorptions of neutral ruthenium dinitrogen complexes have been observed for Ru(NN) (2044.9 cm^{-1}), Ru(NN)$_2$ (2093.4 cm^{-1}), Ru(NN)$_3$ (2121.2 cm^{-1}), Ru(NN)$_4$ (2132.8 cm^{-1}), and Ru(NN)$_5$ (2153.8 cm^{-1}), respectively, which about 10, 16, 30, 6, and 5 cm^{-1} blueshifted from the argon matrix counterparts.[20] New absorption at 1942.0 cm^{-1} has also been captured and is characterized to the anionic Ru(NN)$_2^-$ complex. The Ru(NN)$_2^-$ anion is predicted to have $^2\Pi$ ground states with $D_{\infty h}$ symmetry. The asymmetric N–N stretching frequency in the Ru(NN)$_2^-$ anion is calculated to be 1991.7 cm^{-1}, consistent with the experimental value of 1942.0 cm^{-1}.

B. NN*M*CO (*M*=Ru,Rh)

In the Ru+CO+N$_2$ experiments, new bands at 2116.0 and 1962.6 cm^{-1} appear together during sample deposition, increase upon sample annealing, slightly decrease after broadband irradiation, and slightly increase after further annealing to higher temperature (Table I and Fig. 3). The lower band at 1962.6 cm^{-1} shifts to 1918.4 cm^{-1} with $^{13}C^{16}O$ and to 1919.9 cm^{-1} with $^{12}C^{18}O$, exhibiting isotopic frequency ratios ($^{12}C^{16}O/^{13}C^{16}O$: 1.0230; $^{12}C^{16}O/^{12}C^{18}O$: 1.0222) characteristic of C–O stretching vibrations. The mixed $^{12}C^{16}O+^{13}C^{16}O+N_2$ (Fig. 4, trace c) and $^{12}C^{16}O+^{12}C^{18}O+N_2$ (Fig. 4, trace e) isotopic spectra only provide the sum of pure isotopic bands, implying that one CO unit is involved in this mode.[28] The 1962.6 cm^{-1} band is about 27 cm^{-1} blueshifted from the C–O stretching vibrational frequency in RuCO (Table I).[17] Furthermore, the 1962.6 cm^{-1} band also shows a small shift with $^{15}N_2$ (2.2 cm^{-1}) (Table I and Fig. 4), suggesting that the N$_2$ unit is involved in this complex. The upper band at 2116.0 cm^{-1} shows very small shifts with $^{13}C^{16}O$ and $^{12}C^{18}O$ ($^{12}C^{16}O/^{13}C^{16}O$: 1.0005; $^{12}C^{16}O/^{12}C^{18}O$: 1.0005) but a large shift with $^{15}N_2$ ($^{14}N_2/^{15}N_2$: 1.0325), indicating that this mode is mainly due to a N–N stretching vibration. The mixed CO+$^{14}N_2$+$^{15}N_2$ isotopic spectra (Fig. 4, trace g) only provide the sum of pure isotopic bands, which indicate only one N$_2$ unit is involved in the complex.[28] The 2116.0 cm^{-1} band is about 71 cm^{-1} blueshifted from the N–N stretching vibrational frequency in RuNN (Table I). Accordingly, the absorptions at 2116.0 and 1962.6 cm^{-1} are assigned to the N–N and C–O stretching modes of NNRuCO (marked 9), respectively. The corresponding absorptions of the N–N and C–O stretching modes of the [Ru^{II}(CO)(N$_2$)]$^{2+}$ complex have been observed at 2218 and 2023 cm^{-1} on yttrium zeolite,[29] respectively, which are about 102 and 60 cm^{-1} blueshifted from the neon matrix counterpart of NNRuCO.

In the Rh+CO+N$_2$ experiments, similar absorptions at 2230.0 and 2006.9 cm^{-1} have been observed (Table II and Figs. 5 and 6), which are assigned to the N–N and C–O stretching vibrations of NNRhCO (marked **9′**), respectively. Briefly, the 2006.9 cm^{-1} band shifts to 1961.5 cm^{-1} with $^{13}C^{16}O$, to 1962.3 cm^{-1} with $^{12}C^{18}O$, and to 2005.9 cm^{-1} with $^{15}N_2$, giving the $^{12}C^{16}O/^{13}C^{16}O$, $^{12}C^{16}O/^{12}C^{18}O$, and $^{14}N_2/^{15}N_2$ frequency ratios of 1.0231, 1.0227, and 1.0005 (Table II), respectively. The 2230.0 cm^{-1} band shifts to 2156.5 cm^{-1} with $^{15}N_2$ (Table II). It is noted that the N–N stretching vibrational frequency of NNRhCO is about 66 cm^{-1} blueshifted from that of RhNN (Table II),[22] and the C–O stretching vibrational frequency of NNRhCO is about 17 cm^{-1} redshifted from that of RhCO (Table II),[18,19] respectively. Previously, the N–N and C–O stretching vibrations of

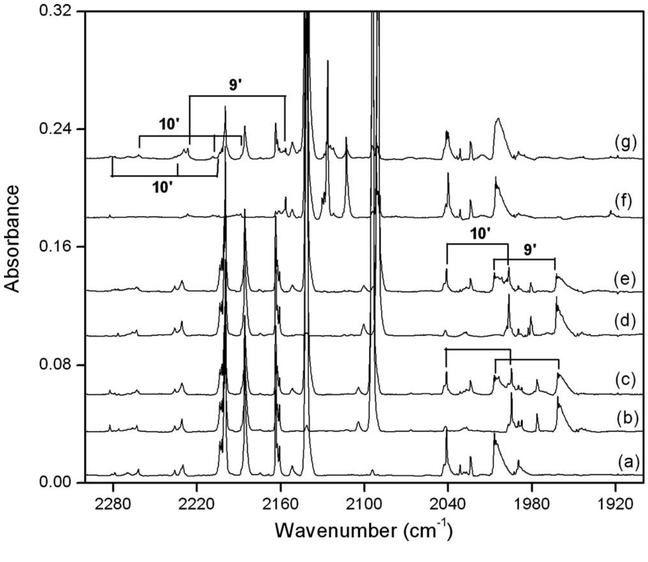

FIG. 6. Infrared spectra in the 2280–1920 cm^{-1} region for laser-ablated Rh atoms codeposited with isotopic CO/N$_2$ mixtures in Ne after annealing to 10 K. (a) 0.1%CO+0.4%N$_2$, (b) 0.1%^{13}CO+0.4%N$_2$, (c) 0.06%^{12}CO+0.06%^{13}CO+0.4%N$_2$, (d) 0.1%C^{18}O+0.4%N$_2$, (e) 0.06%C^{16}O+0.06%C^{18}O+0.4%N$_2$, (f) 0.1%CO+0.4% ^{15}N$_2$, and (g) 0.1%CO+0.3% ^{14}N$_2$+0.3% ^{15}N$_2$.

TABLE I. IR Absorptions (in cm^{-1}) observed from codeposition of laser-ablated Ru atoms with CO and N_2 mixtures in excess neon at 4 K.

$CO+N_2$	$^{13}CO+N_2$	$C^{18}O+N_2$	$CO+^{15}N_2$	$R(^{12}CO/^{13}CO)$	$R(C^{16}O/C^{18}O)$	$R(^{14}N/^{15}N)$	Assignment
2222.0	2220.9	2220.9	2150.5	1.0005	1.0005	1.0332	$NNRu(CO)_2$ (**11**)
2215.5	2214.8	2215.1	2142.6	1.0003	1.0002	1.0340	$(NN)_2RuCO$ (**10**)
2163.9	2163.9	2163.9	2092.0	1.0000	1.0000	1.0344	$(NN)_2RuCO$ (**10**)
2153.5	2153.5	2153.5	2082.0	1.0000	1.0000	1.0343	$Ru(NN)_5$ (**7**)
2132.8	2132.8	2132.8	2061.7	1.0000	1.0000	1.0345	$Ru(NN)_4$ (**6**)
2121.2	2121.2	2121.2	2050.5	1.0000	1.0000	1.0345	$Ru(NN)_3$ (**5**)
2116.0	2114.9	2114.9	2049.3	1.0005	1.0005	1.0325	NNRuCO (**9**)
2093.4	2093.4	2093.4	2023.8	1.0000	1.0000	1.0344	$Ru(NN)_2$ (**4**)
2044.9	2044.9	2044.9	1977.1	1.0000	1.0000	1.0343	RuNN (**3**)
2024.4	1978.2	1981.3	2022.1	1.0234	1.0218	1.0011	$NNRu(CO)_2$ (**11**)
1985.9	1941.0	1942.7	1983.9	1.0231	1.0222	1.0010	$(NN)_2RuCO$ (**10**)
1972.2	1928.0	1929.3	1967.3	1.0229	1.0222	1.0025	$NNRu(CO)_2$ (**11**)
1962.6	1918.4	1919.9	1960.4	1.0230	1.0222	1.0011	NNRuCO (**9**)
1954.8	1913.6	1907.9	1954.8	1.0215	1.0246	1.0000	$Ru(CO)_2$ (**2**)
1942.0	1942.0	1942.0	1877.0	1.0000	1.0000	1.0346	$RuNN^-$ (**8**)
1936.0	1890.4	1895.4	1936.0	1.0241	1.0214	1.0000	RuCO (**1**)

the NNRhCO species have been observed at 2234 and 2048 cm^{-1} on an Al_2O_3 surface,[7] which is in accord with the present matrix spectra.

DFT calculations have been performed for the NNRuCO and NNRhCO complexes to support the above assignments. The NNRuCO and NNRhCO complexes are predicted to have $^3\Sigma^-$ and $^2\Sigma^-$ ground states with linear structures (Table III and Fig. 7), respectively. For NNRuCO, the N–N and C–O stretching vibrational frequencies are calculated to be 2300.7 and 2044.0 cm^{-1}, respectively. The bending modes are predicted to be 498.3 cm^{-1} (Table III), in which the intensity (0.3 km/mol) is too small to be detected, consistent with the absence from the experimental observation. The Ru–C stretching mode is calculated to be 466.8 cm^{-1} with the intensity of 57 km/mol. At the B3LYP level, generally, the calculated harmonic frequencies are higher than the experimentally observed anharmonic values. Consequently, the absorption of the Ru–C stretching vibration is expected to appear around 400 cm^{-1}, which is quite close to the detection limitation of current HgCdTe (MCT) detector (spectral range: $5000-400$ cm^{-1}) and readily to be coupled by the noise, thus resulting in the difficulty in detecting the Ru–C stretching mode. For the C–O stretching mode of the NNRuCO complex, the calculated $^{12}C^{16}O/^{13}C^{16}O$, $^{12}C^{16}O/^{12}C^{18}O$, and $^{14}N/^{15}N$ isotopic frequency ratios of 1.0233, 1.0229, and 1.0018 (Table IV) are consistent with the experimental observations, 1.0230, 1.0222, and 1.0011, respectively. The calculated $^{12}C^{16}O/^{13}C^{16}O$, $^{12}C^{16}O/^{12}C^{18}O$, and $^{14}N/^{15}N$ isotopic frequency ratios of the N–N stretching mode of the NNRuCO complex also agree with the experimental values (Table IV). Similar results have also been obtained for the NNRhCO complex (Tables III and IV and Fig. 7). Previous calculation of the bent NNRhCO complex predicted the N–N and C–O stretching vibrational frequencies at 2293 and 2053 cm^{-1}.[13]

C. $(NN)_2MCO$ (M=Ru,Rh)

In the $Ru+CO+N_2$ experiments, new bands at 2215.5, 2163.9, and 1985.9 cm^{-1} appear together during sample deposition, increase upon sample annealing, visibly increase after broadband irradiation, and slightly increase after further annealing to higher temperature (Table I and Fig. 3). The lower band at 1985.9 cm^{-1} shifts to 1941.0 cm^{-1} with $^{13}C^{16}O$ and to 1942.7 cm^{-1} with $^{12}C^{18}O$, exhibiting isotopic frequency ratios ($^{12}C^{16}O/^{13}C^{16}O$: 1.0231; $^{12}C^{16}O/^{12}C^{18}O$: 1.0222) characteristic of C–O stretching vibrations. The mixed $^{12}C^{16}O+^{13}C^{16}O+N_2$ (Fig. 4, trace c) and $^{12}C^{16}O$

TABLE II. IR absorptions (in cm^{-1}) observed from codeposition of laser-ablated Rh atoms with CO and N_2 mixtures in excess neon at 4 K.

$CO+N_2$	$^{13}CO+N_2$	$C^{18}O+N_2$	$CO+^{15}N_2$	$R(^{12}CO/^{13}CO)$	$R(C^{16}O/C^{18}O)$	$R(^{14}N/^{15}N)$	Assignment
2278.9	2278.9	2278.9	2204.4	1.0000	1.0000	1.0338	$(NN)_2RhCO$ (**10′**)
2262.0	2263.2	2263.3	2188.7	0.9995	0.9994	1.0335	$(NN)_2RhCO$ (**10′**)
2230.0	2230.9	2230.9	2156.5	0.9996	0.9996	1.0341	NNRhCO (**9′**)
2199.7	2199.7	2199.7	2126.3	1.0000	1.0000	1.0345	$Rh(NN)_2$ (**4′**)
2185.8	2185.8	2185.8	2113.0	1.0000	1.0000	1.0345	$Rh(NN)_3$ (**5′**)
2163.6	2163.6	2163.6	2091.6	1.0000	1.0000	1.0344	RhNN (**3′**)
2041.2	1994.6	1996.5	2040.0	1.0234	1.0224	1.0006	$(NN)_2RhCO$ (**10′**)
2031.5	1987.2	1982.7	2031.5	1.0223	1.0246	1.0000	$Rh(CO)_2$ (**2′**)
2023.9	1976.3	1980.7	2023.9	1.0241	1.0218	1.0000	RhCO (**1′**)
2006.9	1961.5	1962.3	2005.9	1.0231	1.0227	1.0005	NNRhCO (**9′**)
1989.6	1989.6	1989.6	1923.5	1.0000	1.0000	1.0344	$Rh(NN)_2^-$ (**8′**)

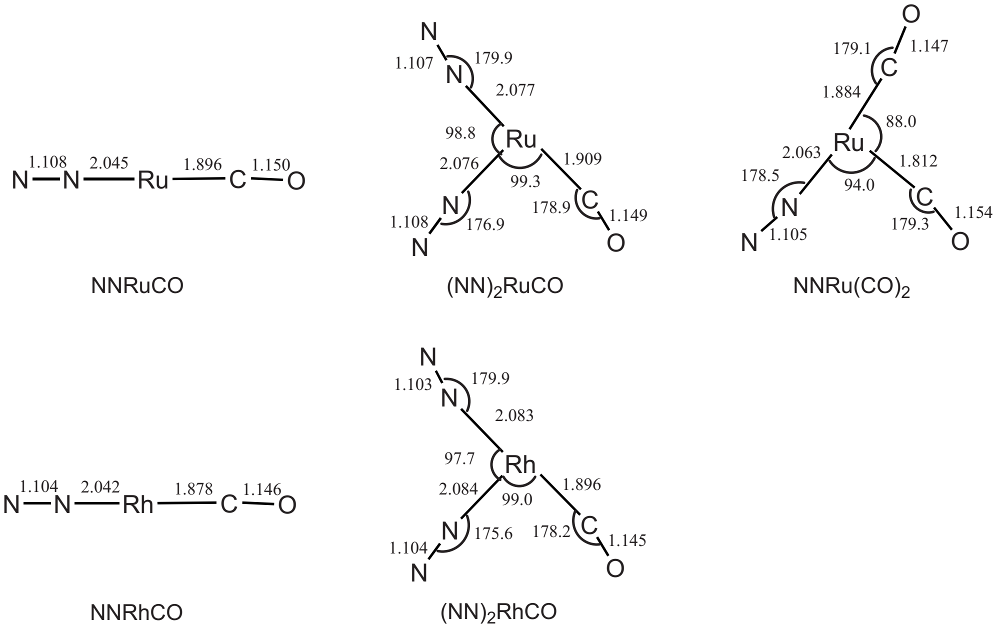

FIG. 7. Optimized structures (bond lengths in angstrom, bond angles in degree) of the new reaction products.

$+{}^{12}C^{18}O+N_2$ (Fig. 4, trace e) isotopic spectra only provide the sum of pure isotopic bands, implying that one CO unit is involved in this mode.[28] It is noted that the 1985.9 cm^{-1} band is about 50 cm^{-1} blueshifted from the C–O stretching vibrational frequency in RuCO (Table I).[17] Furthermore, the 1985.9 cm^{-1} band also shows a small shift with ${}^{15}N_2$ (Table I and Fig. 4), suggesting that the N_2 unit is involved in this complex. The upper two bands at 2215.5 and 2163.9 cm^{-1} show large shifts with ${}^{15}N_2$ (${}^{14}N_2/{}^{15}N_2$: 1.0340 and 1.0344), indicating that these modes are mainly due to N–N stretching vibration, respectively. Two sets of triplet isotopic pattern are observed in the mixed $CO+{}^{14}N_2+{}^{15}N_2$ isotopic spectra (Fig. 4, trace g), which indicate two equivalent N_2 units are involved in the complex.[28] On the other hand, the stronger 2163.9 cm^{-1} band is about 71 cm^{-1} blueshifted from the asymmetric N–N stretching vibrational frequency in $Ru(NN)_2$ (Table I).[20] Accordingly, the absorptions at 2215.5, 2163.9, and 1985.9 cm^{-1} are assigned to the symmetric and

TABLE III. Calculated ground electronic states, point groups, vibrational frequencies (cm^{-1}), and intensities (km/mol) of the new products.

Species	Ground electronic state	Point group	Frequency (intensity, mode)
NNRuCO	${}^3\Sigma^-$	$C_{\infty v}$	2300.7 (353, σ), 2044.0 (1664, σ), 498.3 (0.3×2, π), 466.8 (57, σ), 330.1 (72, σ), 293.9 (0.1×2, π), 63.4 (1×2, π)
$(NN)_2RuCO$	${}^3A'$	C_s	2306.1 (252, A′), 2277.1 (580, A′), 2040.9 (1461, A′), 505.7 (12, A′), 451.2 (52, A′), 451.2 (0.1, A″), 322.8 (1, A′), 300.9 (52, A′), 267.8 (17, A′), 266.8 (0.1, A″), 253.7 (1, A′), 187.5 (1, A″), 73.4 (1, A′), 65.6 (1, A″), 61.7 (0.1, A′)
$NNRu(CO)_2$	${}^1A'$	C_s	2326.9 (258, A′), 2082.3 (1205, A′), 2020.1 (1053, A′), 646.5 (15, A′), 553.9 (10, A), 489.2 (15, A′), 463.5 (21, A′), 449.3 (2, A″), 417.2 (5, A″), 319.4 (26, A′), 292.8 (28, A′), 287.0 (0.4, A″), 103.4 (1, A′), 75.9 (0.3, A′), 29.6 (2, A″)
NNRhCO	${}^2\Sigma^-$	$C_{\infty v}$	2338.3 (264, σ), 2076.5 (1416, σ), 457.3 (57, σ), 443.6 (1×2, π), 312.5 (61, σ), 269.4 (0.01×2, π), 45.0 (1×2, π)
$(NN)_2RhCO$	${}^2A'$	C_s	2345.7 (208, A′), 2320.6 (368, A′), 2074.4 (1257, A′), 461.9 (4, A′), 437.1 (54, A′), 356.4 (2, A″), 286.1 (1, A′), 277.2 (44, A′), 242.7 (13, A′), 228.9 (0.1, A″), 211.3 (1, A′), 159.1 (0.1, A″), 68.5 (0.4, A′), 58.4 (0.03, A′), 39.9 (1, A″)

TABLE IV. Comparison of experimental and calculated IR frequency ratios for the new products.

	Freq (cm^{-1})			$R(^{12}CO/^{13}CO)$		$R(C^{16}O/C^{18}O)$		$R(^{14}N/^{15}N)$	
Species	expt	calcd	Mode	expt	calcd	expt	calcd	expt	calcd
NNRuCO	2116.0	2300.7	ν_{N-N}	1.0005	1.0005	1.0005	1.0003	1.0325	1.0340
	1962.6	2044.0	ν_{C-O}	1.0230	1.0233	1.0222	1.0229	1.0011	1.0009
$(NN)_2RuCO$	2215.5	2306.1	ν_{N-N}	1.0005	1.0003	1.0005	1.002	1.0340	1.0344
	2163.9	2277.1	ν_{N-N}	1.0000	1.0000	1.0000	1.0000	1.0344	1.0350
	1985.9	2040.9	ν_{C-O}	1.0231	1.0233	1.0222	1.0232	1.0010	1.0006
$NNRu(CO)_2$	2222.0	2326.9	ν_{N-N}	1.0003	1.0005	1.0002	1.0003	1.0340	1.0340
	2024.4	2082.3	ν_{C-O}	1.0234	1.0238	1.0218	1.0221	1.0011	1.0010
	1972.2	2020.1	ν_{C-O}	1.0229	1.0240	1.0222	1.0227	1.0025	1.0000
NNRhCO	2230.0	2338.3	ν_{N-N}	0.9996	1.0003	0.9996	1.0002	1.0341	1.0343
	2006.9	2076.5	ν_{C-O}	1.0231	1.0234	1.0227	1.0231	1.0005	1.0007
$(NN)_2RhCO$	2278.9	2345.7	ν_{N-N}	1.0000	1.0002	1.0000	1.0001	1.0338	1.0346
	2262.0	2320.6	ν_{N-N}	0.9995	1.0000	0.9994	1.0000	1.0335	1.0350
	2041.2	2074.4	ν_{C-O}	1.0234	1.0234	1.0224	1.0234	1.0006	1.0004

asymmetric N–N and C–O stretching modes of $(NN)_2RuCO$ (marked 10), respectively. The corresponding absorptions of the symmetric and asymmetric N–N and C–O stretching modes of the $[Ru^{II}(CO)_2(N_2)]^{2+}$ complex have been observed at 2231, 2129, and 2061 cm^{-1} on yttrium zeolite,[29] respectively.

In the Rh+CO+N_2 experiments, similar absorptions at 2278.9, 2262.0, and 2041.2 cm^{-1} have been observed (Table II and Figs. 5 and 6), which are assigned to the symmetric and asymmetric N–N and C–O stretching vibrations of $(NN)_2RhCO$ (marked **10′**), respectively. The 2041.2 cm^{-1} band shifts to 1994.6 cm^{-1} with $^{13}C^{16}O$, to 1996.5 cm^{-1} with $^{12}C^{18}O$, and to 2040.0 cm^{-1} with $^{15}N_2$ giving the $^{12}C^{16}O/^{13}C^{16}O$, $^{12}C^{16}O/^{12}C^{18}O$, and $^{14}N_2/^{15}N_2$ frequency ratios of 1.0234, 1.0224, and 1.0006 (Table II), respectively. The 2262.0 cm^{-1} band shifts to 2188.7 cm^{-1} with $^{15}N_2$ (Table II). The asymmetric N–N stretching vibrational frequency of $(NN)_2RhCO$ is about 62 cm^{-1} blueshifted from that of $Rh(NN)_2$ (Table II),[22] and the C–O stretching vibrational frequency of $(NN)_2RhCO$ is about 17 cm^{-1} blueshifted from that of RhCO (Table II),[18,19] respectively.

The $(NN)_2RuCO$ and $(NN)_2RhCO$ complexes are predicted to have $^3A'$ and $^2A'$ ground states with C_s symmetry (Table III and Fig. 7), respectively. The symmetric and asymmetric N–N and C–O stretching frequencies of the $(NN)_2RuCO$ species are calculated to be 2306.1, 2277.1, and 2040.9 cm^{-1} (Table III), respectively. The calculated $^{12}C^{16}O/^{13}C^{16}O$, $^{12}C^{16}O/^{12}C^{18}O$, and $^{14}N/^{15}N$ isotopic frequency ratios of the asymmetric N–N and C–O stretching vibrations are consistent with the experimental values (Table IV), respectively. Similarly, overall agreement between the experimental and calculated vibrational frequencies, relative absorption intensities, and isotopic shifts supports the identification of the $(NN)_2RhCO$ complex (Tables III and IV and Fig. 7).

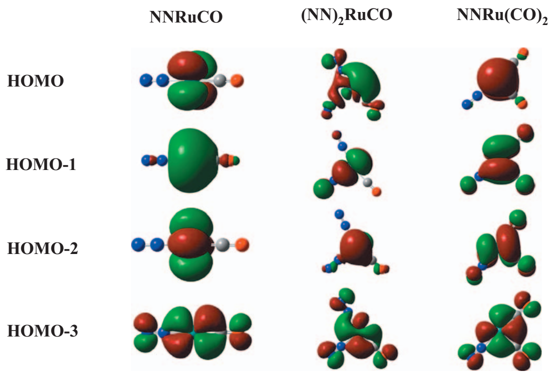

FIG. 8. Molecular orbital pictures of NNRuCO, $(NN)_2RuCO$, and $NNRu(CO)_2$ showing the HOMOs down to the third valence molecular orbital from the HOMO.

D. $NNRu(CO)_2$

In the Ru+CO+N_2 experiments, new bands at 2222.0, 2024.4, and 1972.2 cm^{-1} appear together during sample deposition, sharply increase after broadband irradiation, and slightly decrease after further annealing to higher temperature (Table I and Fig. 3). The upper band at 2222.0 cm^{-1} shows very small shifts with $^{13}C^{16}O$ and $^{12}C^{18}O$ ($^{12}C^{16}O/^{13}C^{16}O$: 1.0005; $^{12}C^{16}O/^{12}C^{18}O$: 1.0005) but a large shift with $^{15}N_2$ ($^{14}N_2/^{15}N_2$: 1.0332), indicating that this mode is mainly due to a N–N stretching vibration. The mixed CO+$^{14}N_2$+$^{15}N_2$ isotopic spectra (Fig. 4, trace g) only provide the sum of pure isotopic bands, which indicates only one N_2 unit is involved in the complex.[28] The lower two bands shift to 1978.2 and 1928.0 cm^{-1} with $^{13}C^{16}O$ and to 1981.3 and 1929.3 cm^{-1} with $^{12}C^{18}O$, exhibiting isotopic frequency ratios ($^{12}C^{16}O/^{13}C^{16}O$: 1.0234 and 1.0229; $^{12}C^{16}O/^{12}C^{18}O$: 1.0218 and 1.0222) characteristic of C–O stretching vibrations. In the mixed isotopic experiments (Fig. 4, traces c and e), two sets of triplet isotopic patterns are observed for these two bands, respectively, suggesting that two equivalent CO units are involved in these modes.[28] Accordingly, the absorptions at 2222.0, 2024.4, and 1972.2 cm^{-1} are assigned to the N–N, symmetric C–O, and asymmetric C–O stretching vibrations of $NNRu(CO)_2$ (marked 11), respectively. The asymmetric C–O stretching vibrations are about 17 cm^{-1} blueshifted from that of the linear $Ru(CO)_2$ (Table I),[17] respectively. The rhodium counterpart, $NNRh(CO)_2$, is absent from the present matrix experiment.

DFT calculation predicts the $NNRu(CO)_2$ complex to have a C_s symmetry (Fig. 7) with a $^1A'$ ground state (Table III). The N–N, symmetric C–O, and asymmetric C–O stretching vibrations are calculated to be 2326.9, 2082.3, and 2020.1 cm^{-1} (Table III), respectively. It can be found from Table IV that the calculated $^{12}C^{16}O/^{13}C^{16}O$, $^{12}C^{16}O/^{12}C^{18}O$, and $^{14}N/^{15}N$ isotopic frequency ratios of the N–N, symmetric C–O, and asymmetric C–O stretching vibrations are in accord with the experimental values, respectively.

E. Reaction pathway and bonding consideration

On the basis of the behavior of sample annealing and irradiation, together with the observed species and calculated stable isomers, a plausible reaction pathway can be proposed as follows. Under the present experimental conditions, laser-ablated ruthenium and rhodium atoms react with CO and N_2 mixtures in the excess neon matrices to produce carbonylmetal dinitrogen species as well as metal carbonyls[17–19] and metal dinitrogen complexes.[20–22] The carbonylmetal dinitrogen complexes may be formed from the reactions of metal carbonyls with N_2 or metal dinitrogen complexes with CO (reactions 3–8). These association reactions are predicted to be exothermic. Furthermore, the reactions of metal dinitrogen complexes with CO are calculated to be exothermic by 52.7 kcal/mol for Ru and 47.9 kcal/mol for Rh (reaction 3) and the reactions of metal carbonyls with N_2 are calculated to be exothermic by 21.0 kcal/mol for Ru and 19.0 kcal/mol for Rh (reaction 4), respectively, suggesting that the formation of the primary NNMCO (M=Ru, Rh) products from the reactions of metal dinitrogen complexes with CO is more energetically favorable than that from the reactions of metal carbonyls with N_2. Similarly, the formation of the $(NN)_2M$CO complexes from the addition of CO to the metal dinitrogen $M(NN)_2$ complexes (reaction 5) is predicted to be more energetically favorable than that from the reactions of the NNMCO complexes with N_2 (reaction 6) and the contribution for the formation of the $NNRu(CO)_2$ complexes from reaction 7 is predicted to be larger than that from reaction 8.

$$Ru + CO \rightarrow Ru(CO)_x (x = 1-5), \tag{1a}$$

$$Rh + CO \rightarrow Rh(CO)_y (y = 1-4), \tag{1b}$$

$$Ru + N_2 \rightarrow Ru(NN)_x (x = 1-5), \tag{2a}$$

$$Rh + N_2 \rightarrow Rh(NN)_y (y = 1-4), \tag{2b}$$

$$MNN + CO \rightarrow NNMCO (M = Ru, Rh), \tag{3}$$

$$MCO + N_2 \rightarrow NNMCO, \tag{4}$$

$$M(NN)_2 + CO \rightarrow (NN)_2MCO, \tag{5}$$

$$NNMCO + N_2 \rightarrow (NN)_2MCO, \tag{6}$$

$$NNRuCO + CO \rightarrow NNRu(CO)_2, \tag{7}$$

$$Ru(CO)_2 + N_2 \rightarrow NNRu(CO)_2. \tag{8}$$

Previous study on the reaction of group 11 metal atoms with CO and O_2 mixture has demonstrated that the reactivity of copper toward CO is prior to O_2, and the reactivity of silver toward O_2 is prior to CO, whereas the reactivity of gold toward CO is comparable to O_2.[30] Present and previous investigations revealed that with the approach of matrix-isolation infrared spectroscopy combined with quantum chemical calculation, the relative reactivity of metal atoms toward different small molecules could be evaluated through exploring the reaction of metal atoms with the mixture of small molecules.

It is noted that the only NNRhCO complex has been hitherto generated on the supported metal surfaces[7,12] and other neutral carbonylmetal dinitrogen complexes captured in the present matrices [i.e., NNRuCO, $(NN)_2$RuCO, $(NN)_2$RhCO, and $NNRu(CO)_2$] are hopefully observed in the future experimental investigations for surface species on metal catalysts.

As illustrated in Fig. 8, the highest occupied molecular orbital (HOMO) and HOMO-2 in the NNRuCO complex are largely Ru 4d in character and the HOMO-1 is of σ-type with the contribution main from the interaction between the atomic orbitals of Ru and molecular orbitals of CO. The degenerate HOMO-3 is of π-type. In the $(NN)_2$RuCO complex, the HOMO and HOMO-3 are of σ-type and the HOMO-1 is of π-type; furthermore, the HOMO-2 is of σ-type with the contribution main from the interaction between the atomic orbitals of Ru and molecular orbitals of CO and N_2. In the $NNRu(CO)_2$ complex, the HOMO is of σ-type with the contribution main from the interaction between the atomic orbitals of Ru and molecular orbitals of CO; the HOMO-1 and HOMO-2 are of π-type and the HOMO-3 is of π-type, in which the contribution main is from the interaction between the atomic orbitals of Ru and molecular orbitals of CO and N_2, respectively.

IV. CONCLUSIONS

Reactions of laser-ablated Ru and Rh atoms with CO and N_2 mixture in excess neon have been studied using matrix isolation infrared spectroscopy. Besides the metal carbonyls and dinitrogen complexes, the carbonylmetal dinitrogen complexes, $(NN)_nM$CO (M=Ru, Rh; n=1, 2) and $NNRu(CO)_2$, are formed during sample deposition or after annealing and are characterized using infrared spectroscopy on the basis of the results of the isotopic substitution and mixed isotopic splitting patterns. DFT calculations have been performed on these complexes. The identifications of these carbonylmetal dinitrogen complexes are confirmed by the overall agreement between the experimental and calculated vibrational frequencies, relative absorption intensities, and isotopic shifts. This study reveals that the reactivity of Ru and Rh atoms toward CO is prior to N_2.

ACKNOWLEDGMENTS

The authors acknowledge the reviewers for their valuable suggestions. This work was supported by AIST and a Grant-in-Aid for Scientific Research (B) (Grant No. 17350012) from the Ministry of Education, Culture, Sports, Science and Technology (MEXT) of Japan. L.J. is grateful to the Japan Society for the Promotion of Science (JSPS) for a postdoctoral fellowship. Z.-H.L. acknowledges JASSO and Kobe University for Honors Scholarship.

[1] See, for example: R. E. Bandy, C. Lakshminarayan, R. K. Frost, and T. S. Zwier, J. Chem. Phys. **98**, 5362 (1993); L. S. Wang, H. S. Cheng, and J. Fan, *ibid.* **102**, 9840 (1995); M. A. Duncan, Int. Rev. Phys. Chem. **22**, 407 (2003).

[2] For example, see: C. Xu, L. Manceron, and J. P. Perchard, J. Chem. Soc., Faraday Trans. **89**, 1291 (1993); V. E. Bondybey, A. M. Smith, and J. Agreiter, Chem. Rev. (Washington, D.C.) **96**, 2113 (1996); S. Fedrigo, T. L. Haslett, and M. Moskovits, J. Am. Chem. Soc. **118**, 5083 (1996); L. Khriachtchev, M. Pettersson, N. Runeberg, J. Lundell, and M. Rasanen, Nature (London) **406**, 874 (2000); H. J. Himmel, L. Manceron, A. J. Downs, and P. Pullumbi, J. Am. Chem. Soc. **124**, 4448 (2002); J. Li, B. E. Bursten, B. Liang, and L. Andrews, Science **295**, 2242 (2002); L. Andrews and X. Wang, *ibid.* **299**, 2049 (2003).

[3] M. F. Zhou, N. Tsumori, Z. Li, K. Fan, L. Andrews, and Q. Xu, J. Am. Chem. Soc. **124**, 12936 (2002); M. F. Zhou, Q. Xu, Z. Wang, and P. R. Schleyer, *ibid.* **124**, 14854 (2002); L. Jiang and Q. Xu, *ibid.* **127**, 42 (2005); Q. Xu, L. Jiang, and N. Tsumori, Angew. Chem., Int. Ed. **44**, 4338 (2005); L. Jiang and Q. Xu, J. Am. Chem. Soc. **127**, 8906 (2005).

[4] *Advanced Inorganic Chemistry*, edited by F. A. Cotton, G. Wilkinson, C. A. Murillo, and M. Bochmann (Wiley, New York, 1999).

[5] E. L. Muetterties and J. Stein, Chem. Rev. (Washington, D.C.) **79**, 479 (1979).

[6] E. A. Wovchko and J. T. Yates, Jr., J. Am. Chem. Soc. **117**, 12557 (1995).

[7] E. A. Wovchko and J. T. Yates, Jr., J. Am. Chem. Soc. **118**, 10250 (1996).

[8] E. A. Wovchko and J. T. Yates, Jr., J. Am. Chem. Soc. **120**, 7544 (1998).

[9] I. A. Fisher and A. T. Bell, J. Catal. **162**, 54 (1996).

[10] T. H. Ballinger and J. T. Yates, Jr., J. Am. Chem. Soc. **114**, 10074 (1992).

[11] A. Erdöhelyi, J. Cserényi, and F. Solyumosi, J. Catal. **141**, 287 (1993).

[12] H. Miessner, J. Chem. Soc., Chem. Commun. **1994**, 927; J. Am. Chem. Soc. **116**, 11522 (1994).

[13] M. L. McKee and S. D. Worley, J. Phys. Chem. A **101**, 5600 (1997).

[14] X. F. Wang and L. Andrews, J. Phys. Chem. A **104**, 9892 (2000).

[15] M. F. Zhou, L. Andrews, and C. W. Bauschlicher, Jr., Chem. Rev. (Washington, D.C.) **101**, 1931 (2001); Y. Gong, M. F. Zhou, and L. Andrews, *ibid.* **109**, 6765 (2009).

[16] H. J. Himmel, A. J. Downs, and T. M. Greene, Chem. Rev. (Washington, D.C.) **102**, 4191 (2002).

[17] M. F. Zhou and L. Andrews, J. Phys. Chem. A **103**, 6956 (1999).

[18] M. F. Zhou and L. Andrews, J. Am. Chem. Soc. **121**, 9171 (1999).

[19] M. F. Zhou and L. Andrews, J. Phys. Chem. A **103**, 7773 (1999).

[20] A. Citra and L. Andrews, J. Phys. Chem. A **104**, 1152 (2000).

[21] A. Citra and L. Andrews, J. Phys. Chem. A **103**, 3410 (1999).

[22] X. F. Wang and L. Andrews, J. Phys. Chem. A **106**, 2457 (2002).

[23] T. R. Burkholder and L. Andrews, J. Chem. Phys. **95**, 8697 (1991); M. F. Zhou, N. Tsumori, L. Andrews, and Q. Xu, J. Phys. Chem. A **107**, 2458 (2003); L. Jiang and Q. Xu, J. Chem. Phys. **122**, 034505 (2005); L. Jiang, Y. L. Teng, and Q. Xu, J. Phys. Chem. A **110**, 7092 (2006).

[24] M. J. Frisch, G. W. Trucks, H. B. Schlegel *et al.*, GAUSSIAN 03, revision B.04, Gaussian, Inc., Pittsburgh, PA, 2003.

[25] (a) C. Lee, W. Yang, and R. G. Parr, Phys. Rev. B **37**, 785 (1988); (b) A. D. Becke, J. Chem. Phys. **98**, 5648 (1993).

[26] A. D. McLean and G. S. Chandler, J. Chem. Phys. **72**, 5639 (1980); R. Krishnan, J. S. Binkley, R. Seeger, and J. A. Pople, *ibid.* **72**, 650 (1980); M. J. Frisch, J. A. Pople, and J. S. Binkley, *ibid.* **80**, 3265 (1984).

[27] D. Andrae, U. Haeussermann, M. Dolg, H. Stoll, and H. Preuss, Theor. Chim. Acta **77**, 123 (1990).

[28] J. H. Darling and J. S. Ogden, J. Chem. Soc. Dalton Trans. **1972**, 2496.

[29] H. Miessner and K. Richter, J. Mol. Catal. A: Chem. **146**, 107 (1999).

[30] Q. Xu and L. Jiang, J. Phys. Chem. A **110**, 2655 (2006).